

## SPECTRAL EVOLUTION OF THE 2010 SEPTEMBER GAMMA-RAY FLARE FROM THE CRAB NEBULA

V. VITTORINI<sup>1</sup>, M. TAVANI<sup>1,2</sup>, G. PUCELLA<sup>3</sup>, E. STRIANI<sup>2</sup>, I. DONNARUMMA<sup>1</sup>, P. CARAVEO<sup>4</sup>, A. GIULIANI<sup>4</sup>, S. MEREGHETTI<sup>4</sup>,  
A. PELLIZZONI<sup>5</sup>, A. TROIS<sup>1,5</sup>, A. FERRARI<sup>6,7</sup>, G. BARBIELLINI<sup>8</sup>, A. BULGARELLI<sup>9</sup>, P. W. CATTANEO<sup>10</sup>, S. COLAFRANCESCO<sup>11</sup>,  
E. DEL MONTE<sup>1</sup>, Y. EVANGELISTA<sup>1</sup>, F. LAZZAROTTO<sup>1</sup>, L. PACCIANI<sup>1</sup>, M. PILIA<sup>12</sup>, AND C. PITTORI<sup>11</sup>

<sup>1</sup> INAF/IASF-Roma, I-00133 Roma, Italy

<sup>2</sup> Dipartimento di Fisica, Università Tor Vergata, I-00133 Roma, Italy

<sup>3</sup> ENEA Frascati, Via Enrico Fermi 45, I-00044 Frascati (Roma), Italy

<sup>4</sup> INAF/IASF-Milano, I-20133 Milano, Italy

<sup>5</sup> INAF-Osservatorio Astronomico di Cagliari, località Poggio dei Pini, strada 54, I-09012 Capoterra, Italy

<sup>6</sup> Dipartimento Fisica, Università di Torino, Turin, Italy

<sup>7</sup> Consorzio Interuniversitario Fisica Spaziale, Villa Gualino, I-10133 Torino, Italy

<sup>8</sup> Dipartimento Fisica and INFN Trieste, I-34127 Trieste, Italy

<sup>9</sup> INAF/IASF-Bologna, I-40129 Bologna, Italy

<sup>10</sup> INFN-Pavia, I-27100 Pavia, Italy

<sup>11</sup> ASI Science Data Center, I-00044 Frascati (Roma), Italy

<sup>12</sup> Dipartimento di Fisica, Università dell'Insubria, Via Valleggio 11, I-22100 Como, Italy

Received 2011 March 16; accepted 2011 March 25; published 2011 April 14

### ABSTRACT

Strong gamma-ray flares from the Crab Nebula have been recently discovered by *AGILE* and confirmed by *Fermi-LAT*. We study here the spectral evolution in the gamma-ray energy range above 50 MeV of the 2010 September flare that was simultaneously detected by *AGILE* and *Fermi-LAT*. We revisit the *AGILE* spectral data and present an emission model based on rapid (within 1 day) acceleration followed by synchrotron cooling. We show that this model successfully explains both the published *AGILE* and *Fermi-LAT* spectral data showing a rapid rise and a decay within 2 and 3 days. Our analysis constrains the acceleration timescale and mechanism, the properties of the particle distribution function, and the local magnetic field. The combination of very rapid acceleration, emission well above 100 MeV, and the spectral evolution consistent with synchrotron cooling contradicts the idealized scenario predicting an exponential cutoff at photon energies above 100 MeV. We also consider a variation of our model based on even shorter acceleration and decay timescales, which can be consistent with the published averaged properties.

*Key words:* acceleration of particles – gamma rays: stars – pulsars: individual (CRAB Nebula)

*Online-only material:* color figures

### 1. INTRODUCTION

The Crab Nebula is at the center of the SN1054 supernova remnant and consists of a rotationally powered pulsar interacting with a surrounding nebula through a relativistic particle wind (e.g., Hester 2008). The Crab pulsar is quite powerful (of spin-down luminosity  $L_{\text{PSR}} = 5 \times 10^{38}$  erg s<sup>-1</sup> and spin period  $P = 33$  ms) and is energizing the whole nebula with its wave/particle output. The inner nebula shows distinctive optical and X-ray brightness enhancements (“wisps,” “knots,” and the “anvil” aligned with the pulsar “jet”; Scargle 1969; Hester et al. 1995, 2002; Hester 2008; Weisskopf et al. 2000). These local variations have been attributed to enhancements of the synchrotron emission produced by instabilities and/or shocks in the pulsar wind outflow. However, when averaged over the whole inner region (several arcminutes across), the Crab Nebula has been considered essentially stable and used as a “standard candle” in high-energy astrophysics. The Crab Nebula X-ray continuum and gamma rays up to ~100 MeV energies are modeled by synchrotron radiation of accelerated particles in an average nebular magnetic field  $\bar{B} = 200 \mu\text{G}$  (Hester et al. 2002; de Jager et al. 1996; Atoyan & Aharonian 1996; Meyer et al. 2010). Emission from GeV to TeV energies is interpreted as inverse Compton radiation by electrons/positrons scattering cosmic microwave background and nebular soft photons (de Jager & Harding 1992; de Jager et al. 1996; Atoyan & Aharonian 1996; Meyer et al. 2010).

Decades of theoretical modeling of this system (e.g., Rees & Gunn 1974; Kennel & Coroniti 1984; de Jager & Harding 1992; de Jager et al. 1996; Atoyan & Aharonian 1996; Arons 2008; Meyer et al. 2010) offer the picture of a remarkable nebular system energized by an MHD pulsar wind interacting with the environment through a sequence of “shocks” or dissipation features localized at distances larger than a few times  $10^{17}$  cm. Efficient particle acceleration at the pulsar wind termination shock regions is believed to be occurring either through diffusive processes, e.g., (Blandford & Eichler 1987; de Jager & Harding 1992; de Jager et al. 1996; Atoyan & Aharonian 1996), shock-drift acceleration (e.g., Begelman & Kirk 1990), or ion-mediated acceleration (e.g., Arons 2008; Spitkovsky & Arons 2004). Several diffusive acceleration models imply acceleration rates of order of the relativistic electron cyclotron frequency (e.g., de Jager & Harding 1992; de Jager et al. 1996; Atoyan & Aharonian 1996). Assuming equality between the accelerating electric field and the magnetic field at the acceleration site and synchrotron cooling in the cospatial magnetic field leads to a most cited constraint for the maximum radiated photon energy (Aharonian 2004):

$$E_{\gamma, \text{max}} \simeq \frac{9}{4} \alpha^{-1} m_e c^2 \simeq 150 \text{ MeV}, \quad (1)$$

with  $\alpha = e^2/\hbar c$  being the fine structure constant,  $c$  the speed of light, and  $m_e$  the electron’s mass. Equation (1) applies in a natural way to diffusively accelerated particles, and  $E_{\gamma, \text{max}}$  turns

out to be independent of the local magnetic field. According to the assumptions underlying this formula, emission above 100 MeV would be difficult to sustain in the Crab Nebula environment. Indeed, the exponential cutoff shown by the average gamma-ray spectrum in the 10 MeV–10 GeV range supports this idealization (de Jager & Harding 1992; de Jager et al. 1996).

However, the recent discovery by the *AGILE* satellite of a strong gamma-ray flare above 100 MeV from the Crab Nebula in 2010 September (Tavani et al. 2010, 2011) and the confirmation by the *Fermi*-LAT (Buehler et al. 2010; Abdo et al. 2011) substantially change this picture. Three substantial gamma-ray flaring episodes from the Crab Nebula have been announced so far (Tavani et al. 2011, hereafter T11; Abdo et al. 2011, hereafter A11). The flaring activity was detected only in the gamma-ray energy range 100 MeV–a few GeV, and it is attributed to transient nebular unpulsed emission. No global enhancements are seen in other bands, but high spatial resolution optical and X-ray observation by *Hubble Space Telescope* (*HST*) and *Chandra* detected local enhancement in the “anvil” region.

Three features of the 2010 September event are relevant: (1) the event develops within 3 and 4 days (whereas the others last about 2 weeks); (2) the gamma-ray rise time appears to be remarkably short,  $\tau \leq 1$  day (T11); and (3) the flaring gamma-ray spectrum extends well above the limit of Equation (1) (T11; A11). A flare production site in the inner nebula of size  $L \leq 10^{16}$  cm is favored by both the peak isotropic gamma-ray luminosity  $L_p \approx 5 \times 10^{35}$  erg s $^{-1}$  (which implies for a 3%–5% radiation efficiency that about 2%–3% of the total spin-down pulsar luminosity is dissipated at the flaring site) and by the flare rise time of  $\sim 1$  day. We noticed that the “anvil region” (“knot-2” and possibly “knot-1”) in the Crab Nebula (Scargle 1969; Hester 2008) is an excellent flare site candidate also because of its alignment with the relativistic pulsar jet (T11).

A number of important theoretical questions are raised by these detections. However, the published spectra of the 2010 September event are not homogeneous because of different integration times: a 2 day timescale for the *AGILE* data (T11) and a 4 day timescale for the *Fermi*-LAT data. The spectral shapes also appear different. The *AGILE* data are characterized by a hard curved spectral shape with peak photon energy  $E_p$  of the differential power spectrum  $E_p \simeq 300$  MeV (T11; see Figure 1). On the contrary, the *Fermi*-LAT spectrum shows a quasi power-law shape extending up to a few GeV (A11). Without additional analysis, it is not clear whether the two data sets are consistent with each other. In any case, the hardness of the gamma-ray emission and the rapid spectral evolution challenge the idealized scenario underlying Equation (1) (de Jager & Harding 1992; de Jager et al. 1996; Atayan & Aharonian 1996).

The goal of our Letter is twofold: (1) investigate the consistency of the published *AGILE* and *Fermi*-LAT spectral data of the 2010 September event by integrating the *AGILE* data over a 4 day timescale; and (2) study the spectral evolution of a class of synchrotron emission models based on freshly accelerated particles in the inner nebula, and check its validity for both the *AGILE* and *Fermi*-LAT data.

## 2. SPECTRAL DATA ANALYSIS

In order to test whether the *AGILE* and *Fermi*-LAT spectra of the 2010 September event are consistent with each other, it is necessary to consider data with the same integration timescales. In the absence of *Fermi*-LAT spectral data on a 2 day timescale,

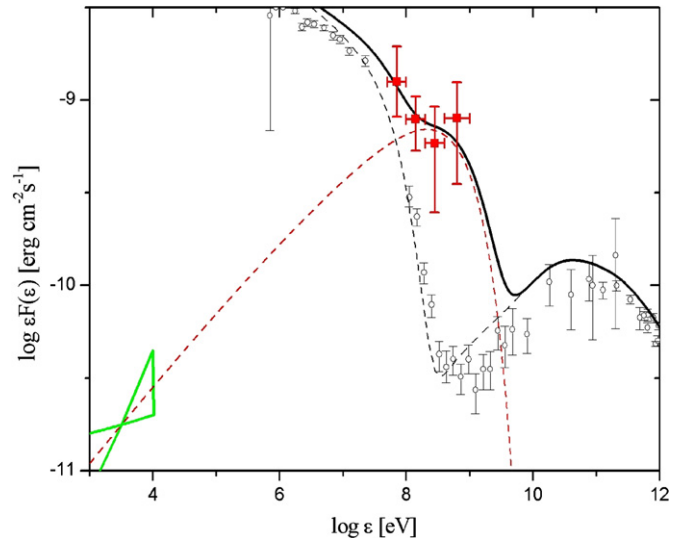


**Figure 1.** *AGILE* (filled squares) 2 day averaged data of the 2010 September gamma-ray flare of the Crab Nebula. Pulsar data have been subtracted. The solid line represents the 2 day averaged synchrotron emission model of the 2010 September flare summed with the standard nebular emission as discussed in the text. The dashed curve in red shows the flaring component averaged over 2 days. Data points in open circles give the standard average Crab Nebula spectrum that we model by the dashed black curve. The spectral region marked in green shows the X-ray data of “source A” of T11.

(A color version of this figure is available in the online journal.)

we revisited our *AGILE* data and carried out a 4 day integration which overlaps with the *Fermi*-LAT interval.

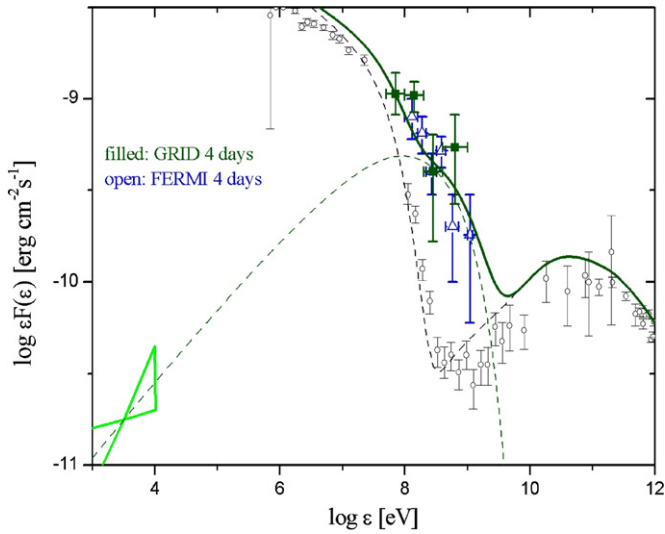
The *AGILE* 4 day Crab spectrum in the energy range 50 MeV–3 GeV was obtained by integrating between MJD 55457.38 and 55461.55. We obtained the nebular contribution by subtracting from the total emission the pulsar contribution corresponding to a flux  $F(E > 100 \text{ MeV}) = 210 \pm 30$  photons cm $^{-2}$  s $^{-1}$  characterized by a power-law spectrum with photon index  $\Gamma = 2.0 \pm 0.1$  in the energy range 50 MeV–3 GeV.

Figure 2 shows the result of our additional analysis of the *AGILE* data together with the published *Fermi*-LAT data. The two data sets are now temporally homogeneous and appear to be in agreement within the errors. The apparent power-law behavior of the 4 day spectrum in the energy range 50 MeV–2 GeV can be explained by a fast-rise-synchrotron-cooling model (see below). The solid curve of Figure 2 shows the result of our modeling for a 4 day average of the rapidly varying spectrum.

## 3. A FAST-RISE-SYNCHROTRON-COOLING MODEL

We assume that a fresh population of impulsively accelerated electrons/positrons is produced in the inner nebula within a timescale short compared with all other relevant cooling timescales. The model presented here has general validity and does not depend on a specific site in the nebula as long as the general characteristics of the emission fit our assumptions. We assume an efficient particle acceleration mechanism<sup>13</sup> that applies simultaneously in one or more contiguous nebular sites that are subject to plasma instabilities and/or substantial pulsar wind particle density enhancements. A fraction of the total volume of the inner nebula is affected by the flaring instability. Consequently, only a fraction of the total number of radiating

<sup>13</sup> We leave for other investigations the crucial issue of explaining the type of plasma wave turbulence leading to the short acceleration timescale (1 day or shorter).



**Figure 2.** *AGILE* (filled squares) and *Fermi*-LAT (open triangles) 4 day averaged spectral data of the 2010 September gamma-ray flare of the Crab Nebula. Pulsar data have been subtracted. The solid line represents the 4 day averaged synchrotron emission model of the 2010 September flare summed with the standard nebular emission as discussed in the text. The dashed curve in green shows the flaring component averaged over 4 days. Data points in open circles give the standard average Crab Nebula spectrum that we model by the dashed black curve.

(A color version of this figure is available in the online journal.)

nebulary particles contribute to the flare. This fact follows from the observed short flaring rise time. For simplicity, we assume a Doppler factor  $\mathcal{D} = (1 - \beta \cos \theta)^{-1} \sim 1$ ; a larger Doppler factor would imply a smaller particle number  $N_e \propto \mathcal{D}^{-3}$ , a larger emitting region  $L \propto \mathcal{D}$ , and smaller rest-frame particle energies  $\gamma \propto \mathcal{D}^{-1/2}$ .

In our analysis we considered different values of the local magnetic field  $B_{\text{loc}}$ . The rapid observed cooling (2 and 3 days) for reasonable values of particle energies implies that the local magnetic field is substantially enhanced compared with  $\bar{B}$  (T11; A11). Reconciling the synchrotron-cooling timescale  $\tau_s \sim (8 \times 10^8 \text{ s}) B_{\text{loc}}^{-2} \gamma^{-1}$  (where the local magnetic field  $B_{\text{loc}}$  is in Gauss and  $\gamma$  is a typical particle Lorentz factor) with the 2010 September observations implies, for  $\gamma \approx 5 \times 10^9$  of electrons irradiating in the GeV range, a local magnetic field  $B_{\text{loc}} \approx 10^{-3} \text{ G}$  that is  $\sim 5$  times larger than the nebular average.

Our best modeling assumes an emitting region of size  $L = 7 \times 10^{15} \text{ cm}$  and an enhanced local magnetic field  $B_{\text{loc}} = 10^{-3} \text{ G}$  that we keep constant in our calculations. The acceleration process produces, within a timescale shorter than any other relevant timescale, a particle energy distribution that we model as a double power-law distribution (T11)

$$\frac{dn}{d\gamma} = \frac{K \gamma_b^{-1}}{(\gamma/\gamma_b)^{p_1} + (\gamma/\gamma_b)^{p_2}}, \quad (2)$$

where  $n$  is the particle number density. The assumption  $\mathcal{D} \sim 1$  together with the constraint on  $B_{\text{loc}}$  implies a break energy  $\gamma_b$  around  $2 \times 10^9$  and a normalization factor  $K$  around  $5 \times 10^{-10} \text{ cm}^{-3}$ . If the gamma-ray flare is related with the persistent local enhancement detected in the anvil region by *HST* and *Chandra* (T11), we can constrain  $p_1 = 2.1$  and  $p_2 = 2.7$ , with the particle Lorentz factor  $\gamma$  ranging from  $\gamma_{\text{min}} = 10^6$  to  $\gamma_{\text{max}} = 7 \times 10^9$ . The double power-law distribution of Equation (2) implies maximal synchrotron emission between  $\gamma_b$  and  $\gamma_{\text{max}}$  and the total particle number required to explain the flaring episode

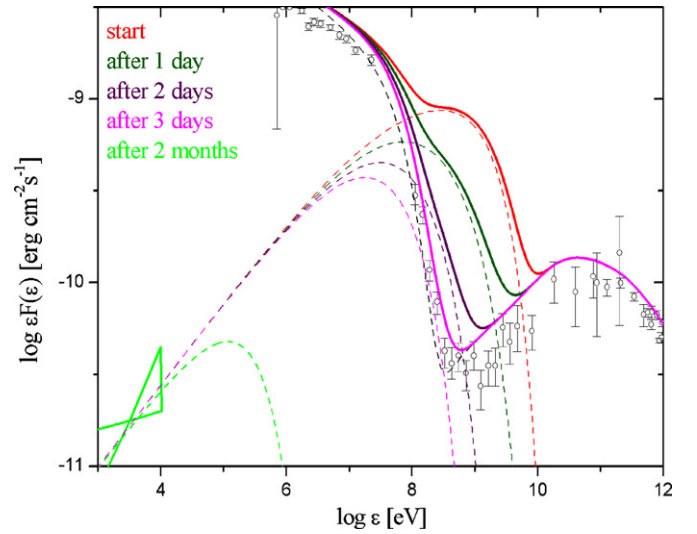


**Figure 3.** Spectral evolution of the gamma-ray Crab Nebula 2010 September flare as obtained by our fast-rise-synchrotron-cooling model. The upper curve shows the spectrum at the starting time and the lower curves show the spectra after 1, 2, 3, and 60 days, respectively. Note the persistence of the X-ray emission in the “source A” of T11 localized by *Chandra*.

(A color version of this figure is available in the online journal.)

turns out to be  $N_{e-/e+} = \int dV (dn/d\gamma) d\gamma = 2 \times 10^{42}$ , where  $V$  is an assumed spherical volume of radius  $L$ . Based on standard synchrotron emissivity and particle cooling, we calculated both the particle distribution and the photon spectrum evolution keeping  $B_{\text{loc}} = 1 \text{ mG}$  constant. We show in Figure 3 the calculated photon spectra at four different times corresponding to days 1–2–3–4. Given our model parameters, fast spectral evolution takes place, and the flaring phenomenon fades away within the fourth day. We also calculated time spectral averages of the differential gamma-ray energy flux  $d\bar{F}/dE$  for different integration time durations  $T$  according to the formula

$$\frac{d\bar{F}}{dE} = T^{-1} \int_0^T \frac{dF}{dE} dt, \quad (3)$$

with the particle energy loss rate  $\dot{\gamma} = -\gamma/\tau_s$  where  $\tau_s$  is the synchrotron-cooling time. We use the time-integrated spectral function of Equation (3) to model the 2 day (Figure 1) and 4 day (Figure 2) integrated spectral data of *AGILE* and *Fermi*-LAT. We find that the synchrotron peak photon energy during day no. 1 is

$$E_{\text{peak}} = \frac{3}{2} \hbar \frac{e B_{\text{loc}}}{m_e c} \gamma_{\text{max}}^2 \simeq 800 \text{ MeV}, \quad (4)$$

which is in good agreement with the peak shown in the 2 day averaged *AGILE* spectrum (Figure 1). In the absence of very strong Doppler effects, our measured spectrum and the calculated  $E_{\text{peak}}$  violate the expectations from Equation (1). Doppler effects with  $\mathcal{D} \sim$  a few would not alter this conclusion. We find that the emission from inverse Compton scattering of the flaring particle population is negligible.

We also note that the spectral shape calculated in Figure 3 and measured in Figure 1 contradicts a simple translation by a Doppler factor of the average nebular data showing the synchrotron burn-off. The additional population of energized particles necessary to explain the flare can be successfully modeled by Equation (2) (that can also account for the X-ray and optical “afterglow” in the anvil region measured by *Chandra* and *HST*; T11).

Our model applies to emitting regions idealized as standing sites or as regions of an MHD flow (such as the anvil enhancements). Adiabatic expansion could play a role in contributing to the gamma-ray flux decrease for an emitting site speed of order of the sound speed. We checked the role of the adiabatic expansion in our model that can explain a good fraction of the observed flux decrease. In this case, our estimate of the local magnetic field  $B_{\text{loc}}$  would be an upper limit. Moreover, there would be no direct relation between the gamma-ray emission and the X-ray emission of the anvil enhancement because, at variance of the synchrotron cooling, adiabatic models cannot account for the persistent brightening in the X-rays (see Figure 3).

We also note that a purely Maxwellian particle energy distribution (presented in T11 and resulting from particle shocks with no non-thermal tails) can also in principle explain the spectral evolution above 100 MeV: also in this case there would be no direct spectral connection between the gamma-ray emission and the X-ray/optical properties of localized regions in the nebula.

#### 4. AN EVEN FASTER EVOLUTION MODEL

In our study, we considered also the possibility of a flux and spectral evolution even faster than that shown in Figures 1–3. The analysis of the *Fermi*-LAT 2010 September data by Balbo et al. (2011) suggests indeed that the spectral evolution may occur on an overall timescale even faster than 1 and 2 days. A cooling timescale of  $\sim 1$  day is explained in our synchrotron model for  $B_{\text{loc}} \sim 2.5$  mG and  $\gamma_{\text{max}} = 5 \times 10^9$ . In this case, the overall flaring episode lasting  $\sim 4$  days is characterized by a sequence of short acceleration and cooling episodes lasting 1 and 2 days. Our analysis remains valid also in presence of a faster evolution. In this case, the magnetic field is determined to have a value  $B_{\text{loc}} \sim 10 \bar{B}$ .

We note that slower events lasting 6 and 7 days, as the 2007 flare presented in (T11), can be interpreted by the same model with larger region involved  $L \approx 5 \times 10^{16}$  cm and similar  $B_{\text{loc}}$ . Determining the gamma-ray temporal structure on timescales shorter than 2 days is limited by photon statistics. The time-resolved analysis of the *AGILE* gamma-ray data for the 2010 September event will be presented elsewhere.

#### 5. DISCUSSION AND CONCLUSIONS

The 2010 September event of the Crab Nebula lasting  $\sim 4$  days is currently the shortest detected gamma-ray flare. Our analysis shows that the flux and spectral evolution of this event are well described by a model characterized by very fast (shorter than  $\sim 1$  day) particle acceleration and by synchrotron cooling in a local magnetic field 5–10 times larger than the average nebular value  $\bar{B}$ . Both the *AGILE* and *Fermi*-LAT gamma-ray spectral data are consistent with each other within a 4 day timescale. Our analysis of the *AGILE* data on a 2 day timescale clearly shows that the emission is peaked at the photon energy of Equation (4), which is almost one order of magnitude larger than the “synchrotron burn-off” constraint of Equation (1). The flaring mechanism in the Crab Nebula is quite remarkable: it accelerates particles to the largest kinetic energies (PeV) associable to a specific astrophysical source and does it within the shortest time ever detected in a nebular environment.

Our results challenge the physical assumptions underlying Equation (1) and in particular acceleration models based on “slow” processes. As we showed above, explanations in terms of Doppler boosting are problematic in light of the measured

spectral curvature of the *AGILE* data. Even though a theoretical study of possible acceleration mechanisms consistent with the data discussed here is beyond the scope of this Letter, we can briefly mention some of the difficulties. First-order *Fermi* acceleration with particles gaining energy by diffusing stochastically back and forth a shock front (e.g., Blandford & Ostriker 1978; Bell 1978; Drury 1983) appears to be too slow and is drastically challenged by our findings. In particular, it is difficult to see how a diffusive shock acceleration mechanism can violate Equation (1). A locally enhanced (over  $B_{\text{loc}}$ ) electric field can produce a sort of “runaway” of kinetic energy gains with an acceleration rate larger than the synchrotron-cooling rate. However, despite some attempts and analogies with other astrophysical contexts (e.g., pulsar magnetospheres), it is currently not clear how this mechanism can be implemented in the Crab Nebula. MHD models of the pulsar wind (e.g., Komissarov & Lyubarsky 2004; Del Zanna et al. 2004; Camus et al. 2009; Komissarov & Lyutikov 2011) address the turbulence and the limit-cycle behavior of the instabilities. These features may in principle favor substantial local magnetic field enhancements. However, the calculated timescales of these instabilities (e.g., Camus et al. 2009) are several orders of magnitudes longer than what we detected in the Crab Nebula. Shock-drift acceleration (Kirk et al. 2000) tends to occur on a timescale shorter than for diffusive processes. However, it is not clear whether the required efficiency can be reached in the flaring Crab Nebula site and whether Equation (4) can be obtained. Shocks mediated by ions in the pulsar wind that resonantly accelerate pairs by magnetosonic waves (Gallant & Arons 1994; Spitkovsky & Arons 2004; Arons 2008) are typically slow and are most likely not applicable in the X-ray and optically enhanced pulsar polar jet regions of T11.

The challenge provided by the Crab Nebula gamma-ray flaring requires a thorough investigation of the mechanisms leading to efficient particle acceleration and to a natural justification of Equation (4). The issue will be elucidated by future *Chandra* X-ray and *HST* optical observations of the inner Crab Nebula that will be carried out in search of the gamma-ray flaring site.

We thank the anonymous referee for his/her comments. Research partially supported by the ASI grant no. I/040/10/0.

#### REFERENCES

- Abdo, A. A., et al. 2011, *Science*, **331**, 739 (A11)
- Aharonian, F. A. 2004, *Very High Energy Cosmic Gamma Radiation* (River Edge, NJ: World Scientific)
- Arons, J. 2008, in *Neutron Stars and Pulsars, 40 Years After the Discovery*, ed. W. Becker (Berlin: Springer), in press (arXiv:0708.1050)
- Atoyan, A. M., & Aharonian, F. A. 1996, *MNRAS*, **278**, 525
- Balbo, M., Walter, R., Ferrigno, C., & Bordas, P. 2011, *A&A*, **527**, L4
- Begelman, M. C., & Kirk, J. C. 1990, *ApJ*, **353**, 66
- Bell, A. R. 1978, *MNRAS*, **182**, 147
- Blandford, R., & Eichler, D. 1987, *Phys. Rep.*, **154**, 1
- Blandford, R., & Ostriker, J. P. 1978, *ApJ*, **221**, L29
- Buehler, R., et al. 2010, *ATel*, **2861**
- Camus, N. F., Komissarov, S. S., Bucciantini, N., & Hughes, P. A. 2009, *MNRAS*, **400**, 1241
- de Jager, O. C., & Harding, A. K. 1992, *ApJ*, **396**, 161
- de Jager, O. C., et al. 1996, *ApJ*, **457**, 253
- Del Zanna, L., Amato, E., & Bucciantini, N. 2004, *A&A*, **421**, 1063
- Drury, L. O. 1983, *Rep. Prog. Phys.*, **46**, 973
- Gallant, Y. A., & Arons, J. 1994, *ApJ*, **435**, 230
- Hester, J. J. 2008, *ARA&A*, **46**, 127
- Hester, J. J., et al. 1995, *ApJ*, **448**, 240
- Hester, J. J., et al. 2002, *ApJ*, **577**, L49

- Kennel, C. F., & Coroniti, F. C. 1984, *ApJ*, **283**, 710
- Kirk, G. J., Guthmann, A. W., Gallant, Y. A., & Achteberg, A. 2000, *ApJ*, **542**, 235
- Komissarov, S. S., & Lyubarsky, Y. E. 2004, *MNRAS*, **349**, 779
- Komissarov, S. S., & Lyutikov, M. 2011, *MNRAS*, in press (arXiv:1011.1800v1)
- Meyer, M., Horns, D., & Zechlin, H. S. 2010, *A&A*, **523**, A2
- Rees, M. J., & Gunn, J. E. 1974, *MNRAS*, **167**, 1
- Scargle, J. D. 1969, *ApJ*, **156**, 401
- Spitkovsky, A., & Arons, J. 2004, *ApJ*, **603**, 669
- Tavani, M., et al. 2010, *ATel*, 2855
- Tavani, M., et al. 2011, *Science*, **331**, 736 (T11)
- Weisskopf, M. C., et al. 2000, *ApJ*, **536**, L81